MiR-195-5p targets CDK1 to regulate new DNA synthesis and inhibit the proliferation of hepatocellular carcinoma cells

Chunhui Zhou
Xiangya Hospital Central South University
Sujuan Zhu
The Tumor Hospital of SUMC, Cancer Hospital of Shantou University Medical College
Haiping Li (haipl0427@163.com)
Xiangya Hospital Central South University

Research Article

Keywords: miR-195-5p, CDK1, HCC, proliferation, cell cycle, DNA damage response

Posted Date: May 5th, 2022

DOI: https://doi.org/10.21203/rs.3.rs-1603605/v1

Abstract

Background

CDK1 is critical for cell viability and plays an important role in biological events. MiR-195 is pivotal in pathogenesis and development of hepatocellular carcinoma (HCC). But the association between CDK1 and miR-195 in HCC is underexplored.

Methods

Gene expression was assayed via qRT-PCR, and corresponding protein levels were assessed via Western blot. Cell cycle was assayed through flow cytometry. DNA replication was detected by EDU staining. Cell proliferation was determined via plate colony formation assay. Targeting relationship between miR-195-5p and CDK1 was analyzed by bioinformatics analysis and dual-luciferase gene assay. DNA damage was marked by immunofluorescence staining.

Results

CDK1 was overexpressed in HCC tissues and cells. Silencing CDK1 modulated cell cycle of HCC cells and inhibited DNA replication and proliferation. In HCC cells, miR-195-5p reduced CDK1 level, inhibited the G1 phase-to-S phase transition, induced DNA damage response, and inhibited DNA replication and proliferation.

Conclusion

MiR-195-5p targeted CDK1 and repressed synthesis of new DNA in HCC cells, thus restraining HCC cell proliferation.

Introduction

Cyclin-dependent kinase (CDK) is an important cell cycle regulating protein. In the CDK family, only CDK1 can foster cell cycle independently[1]. A recent study showed that CDK1 competitively restrains CDK2-cyclin A complex formation, thereby inhibiting re-replication of the replicated DNAs, thus successfully completing the replication in late S phase[2]. In addition to these functions, CDK1 is involved in repair of the double-strand break of homologous recombination (HR) dependent DNA[3] and coupling DNA damage repair pathways to cell cycle processes[4]. Overall, CDK1 is a major modulator of several core biological events.

CDK1 expression is increased in human colorectal cancer[5] and prostate cancer[6]. Thus, CDK1 is involved in tumor progression. Recent studies showed that combination of CDK1 inhibitor JNJ-7706621 and

paclitaxel is effective in treating transplantable liver cancer and repressing tumor growth[7]. However, whether the inhibitory effect of CDK1 on liver cancer progression is related to modulation of cell cycle progression, DNA replication, and DNA damage repair has not been clarified.

Recently, more and more studies have confirmed that microRNA (miRNA) is an essential regulator in many cancers, including hepatocellular carcinoma (HCC)[8]. Studies displayed the decrease of miR-195 in cancers, containing liver cancer, stomach cancer, bladder cancer, breast cancer and adrenocortical cancer[9–12]. The application of miR-195 dramatically constrained HCC cell colony formation *in vitro* and HCC tumor development in nude mice[12]. *In vitro* data showed that miR-195 inhibited tumorgenesis and regulated G1/S transition of HCC cells[9]. Recent studies suggested that miR-195-5p/CDK1 may act as a possible prognostic biomarker and therapeutic target for HCC[13]. But specific biological function and regulatory mechanism of miR-195-5p/CDK1 in HCC are rarely studied.

We unveiled that CDK1 expression was elevated in HCC cells, and miR-195-5p affected cell cycle, DNA replication and DNA damage response via targeting CDK1, thus restraining HCC cell proliferation. CDK1 played a pivotal carcinogenic role in HCC development and progression and is modulated by miR-195-5p. These findings bolstered a better understanding of function of miRNAs in HCC and provided targets for HCC diagnosis and treatment.

1. Materials And Methods

1.1 Bioinformatics analysis

Four sets of HCC mRNA microarray data, including GSE19665 (normal: 10, tumor: 10), GSE25097 (normal: 234, tumor: 268), GSE54236 (normal: 81, tumor: 80), and GSE84402 (normal: 14, tumor: 14) were downloaded from GEO database. Differential analysis between the normal group and the tumor group was performed by R package “limma”. The differential analysis results of the four groups were analyzed by RobustRankAggreg (RRA) package (log|FC|>2, FDR < 0.05) to identify genes that differentially expressed in all the four microarrays.

The “STRING” database was applied to perform protein-protein interaction (PPI) network analysis and calculate the core degree of genes in the network to determine the target mRNA (interaction score: 0.9). Meanwhile, the mature miRNA (normal: 50, tumor: 375), the mRNA expression data (normal: 50, tumor: 374) and the clinical data of HCC were obtained from TCGA-LIHC.

Starbase and TargetScan bioinformatics databases were utilized for predicting miRNAs upstream of target mRNA, and the results were overlapped with the differential miRNAs to obtain the miRNA with binding site with the target mRNA. “Survival” package was utilized for survival analysis and clinical stage analysis of the target mRNA in TCGA-LIHC dataset. GSEA software was applied for pathway enrichment analysis of the target mRNA.

1.2 Cell culture

Human normal liver cells L-02 (CRL-12461) and HCC cell lines, including HepG2 (HB-8065), SNU-398 (CRL-2233) and Hep3b (HB-8064), were all purchased from American Type Culture Collection. These cell lines were maintained in the DMEM (GIBCO BRL, USA) plus 10% FBS (Gibco; Thermo Fisher Scientific, USA) and 1% antibiotics (100 U/mL penicillin and 100 μg/mL streptomycin sulfate) in an incubator at 37 ℃ with 5% CO_2.

1.3 Cell Transfection

MiR-195-5p-mimic, NC-mimic, oe-NC, oe-CDK1, si-CDK1-1, si-CDK1-2 and si-NC were synthesized and provided by GENECHEM (China). According to manufacturer's instructions of Lipofectamine 2000 (Thermo Fisher Scientific, USA), 30 nM mimics, siRNA, oe-RNA and their respective negative controls were transfected into cells.

1.4 Flow cytometry

After being digested, suspended, and rinsed twice with PBS, cells were made into single-cell suspension (1×10^6 cells/mL). The cells were fixed with 70% cold ethanol and then stored at -4°C overnight. Before staining, the cells were rinsed with PBS to remove supernatant. Cells were added with PI/RNase A staining solution (Keygentec, China) and incubated in darkness for 30 min. Flow cytometry was adopted to analyze cells and Flowjo software was utilized to process data. The proportion of cells in different cell cycle phases in each experimental group was compared and analyzed.

1.5 qRT-PCR

RNA in cells was extracted by Trizol Reagent (Thermo Fisher Scientific, USA). The extracted RNA was reversely transcribed into cDNA using the High-Capacity cDNA Reverse Transcription Kit (Thermo Fisher Scientific, USA). According to instructions of the kit, qPCR analysis was done with SYBRA Green PCR Master Mix (Takara, Japan) in QuantStudio 3 (Thermo Fisher Scientific, USA) qPCR instrument (primers: see Table 1). GAPDH was utilized as an internal reference gene for CDK1 expression, and U6 for miR-195-5p.

Table 1
Primers of qRT-PCR

Gene	Primer sequence(5'→ 3')
miR-195-5p	TAGCAGCACAGAAATATTGGC
CDK1	F: GGCTCTGATTGGCTGCTTTG
	R: GGTAGATCCGCGCTAAAGGG
GAPDH	F: AATGGGCAGCCGTTAGGAAA
U6	R: GCGCCCAATACGACCAAATC
	F: UAGCAGCACAGAAAUAUUGGC
	R: AACGCTTCACGAATTTGCGT

1.6 Western blot

RIPA lysis buffer was used to treat cells and isolate intracellular proteins. SDS-polyacrylamide gel electrophoresis was performed on the same amount of protein samples. Then, the proteins were blotted onto the PVDF membrane and sealed with 5% skim milk at room temperature for 1 h. Finally, membrane was co-incubated with primary antibody at 4 ℃ overnight. Antibodies were purchased from Abcam (UK): anti-CDK1 antibody (ab32094), anti-RPA32 antibody (ab109084), anti-p-RPA32 antibody (ab109394), and GAPDH antibody (ab181602). After the primary antibody was washed, membrane was cultured with the secondary antibody IgG H&L (HRP, ab6721) for 1 h at room temperature. Imaging was developed and photographed on ChemiDoc™ Touch Imaging System (Bio-RAD US) using a hypersensitive ECL kit, and finally analyzed using ImageJ.

1.7 EDU Staining

Cells successfully transfected with different plasmids were seeded into 24-well plates (5×10^3 cells per well) with 3 replicates per group. After 12 h of cell culture, the medium of the cells was replaced with 50 μmol/L EDU medium, and the cells were incubated for 2 h in CO_2 incubator. After EDU medium being discarded, cells were fixed with addition of 4% paraformaldehyde for 30 min. Next, 200 μL 2 mg/mL glycine was added, and cells were incubated with a shaker at room temperature for 5 min, followed by PBS washing for 3 times, 5 min each. Subsequently, 300 μL 0.5% Triton X-100 was supplemented, and cells were maintained for 30 min at room temperature. Next, 200 μL Apollo staining solution was supplemented, and cells were maintained at room temperature without light for another 30 min, followed by 0.5% Triton X-100 washing for 3 times, 10 min each. At last, DAPI solution was added for nuclear staining. The staining results were observed under fluorescence microscope. The number of EDU positive cells was counted by ImageJ software.

1.8 Immunofluorescence staining

The transfected cells were inoculated on a slide and treated with 4% formaldehyde solution containing 0.1% TritonX-100 (Sigma, USA) at room temperature for 15 min. After fixation, the slide was blocked with 3% BSA solution (configured with PBS) containing 0.5% TritonX-100 for at least 1 h. After blocking, the slide was maintained with the primary antibodies (anti-γ H2AX antibody ab81299, anti-RPA32 antibody ab109084) at 4 ℃ overnight. Slide was incubated with AlexaFluor488-labeled secondary antibody (Life Technologies, USA) for 1 h at room temperature and stained with DAPI. The automatic Nikon Eclipse Ni microscope with Nikon Elements software (Nikon Instruments) was utilized for imaging and photographs were taken with the 100× oil lens.

1.9 Plate colony formation assay

Cells (logarithmic growth stage) were digested with 0.25% trypsin and blown into single cells. Cells were then suspended in cell growth medium plus 10% FBS for reserve. Each dish in each group was inoculated with 1×10^3 cells and added with 10 mL 37 ℃ pre-heated medium, and the cells were dispersed evenly by gently rotating. The cells were maintained in a 37 ℃ incubator with 5% CO_2 and saturated humidity. The

culture was terminated when visible colonies appeared in the petri dish. The supernatant was discarded and cells were carefully soaked and rinsed twice with PBS. Cells were added with 5 ml of pure methanol and fixed for 15 min. After fixative solution being removed, appropriate amount of crystal violet was added to stain for 20 min, followed by washing off the staining solution slowly with running water and drying in air. A camera was used to photograph, and the number of cell colonies was counted.

1.10 Dual-luciferase reporter assay

The 3'UTR terminal sequences of wild-type and mutant CDK1 were imported into the pMiR-Reporter vectors (Addgene, USA) to construct reporter plasmids. MiR-195-5p-mimic or NC-mimic and the reporter gene plasmid were co-transfected into HepG2, and the fluorescence intensity of transfected groups was assessed through luciferase activity assay kit (Promega, USA) after 24-h culture.

1.11 Data analysis

GraphPad Prism 6 software (GraphPad Software, USA) was utilized for statistical analyses. All experiments were conducted at least 3 times, with results expressed as mean ± SD, and comparisons between groups were carried out using the *t*-test or one-way analysis of variance. $P < 0.05$ meant statistically significant difference, and * in the figure meant $p < 0.05$.

2. Results

2.1 CDK1 may be a target of HCC

A total of 194 differential mRNAs were obtained by the differential analysis of combined gene microarrays. The top 20 up-regulated and top 20 down-regulated differential genes were selected to plot a heat map (Fig. 1A). The degree value of interaction between each gene and other genes was calculated through the PPI network analysis, and it was found that CDK1 was at the core of the whole interaction network, with the highest degree value (Fig. 1B). Analysis of expression levels between the tumor group and the normal group displayed that CDK1 was conspicuously increased in tumor tissues (Fig. 1C). Also, it has been reported that CDK1 is up-regulated in tumor tissues[14]. The survival analysis on the TCGA-LIHC data set illustrated that survival time of patients with overexpressing CDK1 was notably lower than that of patients with decreased CDK1 level (Fig. 1D). It has been documented that CDK1 overexpression has an adverse effect on the prognosis[15]. Based on clinical information of patients, we found that CDK1 had notable differences in different stages of HCC (Fig. 1E). CDK1 level increased with progression of tumor stage in the early stage, but decreased in stage IV. The results of survival analysis displayed that CDK1 may be an oncogene in early HCC *in vivo*.

2.2 CDK1 regulates cell cycle, DNA replication and proliferation of HCC cells

GSEA showed that CDK1 was noticeably enriched in cell cycle and DNA replication pathways (Fig. 2A), which were significantly correlated with cell proliferation. Therefore, in order to explore impact of CDK1 on

cycle and proliferation capacity of HCC cells, we conducted the following experiments. Firstly, CDK1 level in normal human hepatocytes L-02 and HCC cell lines (HepG2, Huh-7, Hep3b) was detected via qRT-PCR. CDK1 was upregulated in HCC cells relevant to normal liver cells (Fig. 2B). As revealed by Western blot, CDK1 protein expression was noticeably enhanced in HCC cell lines relevant to normal human liver cell line. Among them, CDK1 presented the highest expression level in HepG2 cell line (Fig. 2C). Therefore, HepG2 cell line was selected for subsequent experiments. We constructed two CDK1-silenced plasmids and their negative controls. qRT-PCR result showed that si-CDK1-1 had higher transfection efficiency (Fig. 2D). Therefore, we selected si-CDK1-1 for transfection and named it si-CDK1. Flow cytometry results displayed that proportion of G0/G1 phase cells was dramatically increased and that of S phase cells was decreased in si-CDK1 group but not in control group (Fig. 2E). EDU staining results displayed that DNA replication level was decreased in si-CDK1 group in comparison to the control group (Fig. 2F). Cell colony formation unveiled that proliferation level of the si-CDK1 group was remarkably reduced relevant to control group (Fig. 2G). Thus, CDK1 silencing could block process from G0/G1 phase to S phase and inhibit DNA replication, thus inhibiting HCC cell proliferation.

2.3 MiR-195-5p targets and represses CDK1 expression

TarBase and TargetScan bioinformatics databases were utilized to predict upstream miRNAs of CDK1. The predicted results were intersected with differential miRNAs, and 3 differential miRNAs were obtained (Fig. 3A). Pearson correlation analysis was conducted between CDK1 and these 3 miRNAs, and it was found that miR-195-5p had the strongest negative correlation with it (Fig. 3B-C). Expression analysis results of the tumor group and the normal group disclosed that miR-195-5p was noticeably underexpressed in tumor tissues (Fig. 3D). To confirm targeted modulation of miR-195-5p on CDK1, dual-luciferase gene assay was performed. The results showed that fluorescence intensity in WT-CDK1 + miR-195-5p-mimic group was dramatically down-regulated compared with control group. However, there was no notable difference in fluorescence intensity between MUT- CDK1 + miR-195-5p-mimic and the control group, indicating that miR-195-5p targeted CDK1 (Fig. 3E-F). qRT-PCR and Western blot disclosed that enforced miR-195-5p level repressed transcription level and protein expression of CDK1 (Fig. 3G-I). These experimental results indicated that CDK1 was a downstream target gene of miR-195-5p, and miR-195-5p constrained CDK1 expression.

2.4 MiR-195-5p affects cell cycle, DNA replication and proliferation of HCC cells by targeting CDK1

Flow cytometry revealed that in comparison to control group, the proportion of G0/G1 phase cells in the miR-195-5p-mimic + oe-NC group was notably elevated, while the proportion of S phase cells being reduced. However, proportion of cells at G0/G1 phase in the miR-195-5p-mimic + oe-CDK1 group was noticeably inhibited, while proportion of cells at S phase recovered prominently (Fig. 4A). EDU staining unveiled that in comparison to control group, DNA replication level decreased in the miR-195-5p-mimic + oe-NC group, while proportion of DNA replication positive cells recovered in miR-195-5p-mimic + oe-CDK1 group (Fig. 4B). Cell colony formation assay displayed that enforced miR-195-5p level restrained proliferation of HepG2 cell line relevant to control group, while introduction of oe-CDK1 co-transfection

promoted the proliferation of HepG2 cell line (Fig. 4C). Experimental results demonstrated that miR-195-5p affected HCC cell cycle by negatively regulating CDK1, thereby inhibiting DNA replication and reducing the proliferation of HCC cells.

2.5 MiR-195-5p promotes DNA damage response in HCC by targeting CDK1

Studies have shown that CDK1 is involved in DNA damage repair, especially HR-mediated DNA double-strand break repair, and its main role is to promote the terminal resection[3]. Therefore, we set out to investigate whether CDK1-involved DNA damage repair is regulated by miR-195-5p. To this end, immunofluorescence staining was performed to label γH2AX and RPA32 foci. Taking the oe-NC + NC-mimic group as control, DNA damage response was triggered dramatically in miR-195-5p-mimic + oe-NC group, and total fluorescence intensity of γH2AX and RPA32 foci increased significantly. In contrast, the DNA damage response was noticeably downregulated in miR-195-5p-mimic + oe-CDK1 group (Fig. 5A-B). We also revealed that in relevant to oe-NC + NC-mimic group, miR-195-5p-mimic + oe-NC group cells presented excessive phosphorylation of RPA32, which was a marker of the activation of DNA damage response. However, after oe-CDK1 co-transfection, the expression of P-RPA32 protein decreased significantly (Fig. 5C). Hence, miR-195-5p may be a tumor repressor. It promoted DNA damage response in HCC by targeting CDK1, thus constraining HCC cell proliferation.

3. Discussion

Through bioinformatics analysis and cell experiments, we denoted that CDK1 was overexpressed in HCC tissues and cells, which was consistent with results reported previously[16]. We analyzed effect of CDK1 on biological behaviors of HCC and unveiled that CDK1, as an oncogene, affected cell cycle and promoted DNA replication and proliferation of HCC cells. CDK1 has also been reported to be a carcinogenic gene in other cancers. For example, CDK1 is an oncogene whose expression increases with progressive progression of epithelial ovarian cancer[14]. CDK1 level is related to tumor size and grade of pancreatic ductal adenocarcinoma, and patients with increased CDK1 level had a shorter survival time[15]. CDK1 plays an essential role as an oncogene in HCC.

In order to further explore CDK1-related genes, we found the miR-195-5p/CDK1 signaling axis through bioinformatics analysis and that miR-195-5p was dramatically underexpressed in HCC tumor tissues. Meanwhile, we confirmed the miR-195-5p/CDK1 targeting relationship and the repression of CDK1 level by miR-195-5p. hsa-miR-195-5p overexpression in HCC cells reduces PHF19 level, thereby inhibiting malignant behaviors of hepatocytes *in vitro*[17]. Consistent with it, we manifested that miR-195-5p blocked transition of cell cycle from G1 phase to S phase by targeting CDK1 and constraining CDK1 level, thus inhibiting the DNA replication of HCC cells and proliferation of HCC cells.

CDK1 is significantly pluripotent. In addition to regulating cell cycle, it also participates in DNA damage repair and activation of CHK1-dependent cell cycle checkpoints by phosphorylation of BRCA1[18]. To

investigate impact of miR-195-5p/CDK1 on DNA damage repair in HCC cells, immunofluorescence experiments were conducted. It was found that miR-195-5p induced significant DNA damage response by targeting CDK1, and the expression of p-RPA32 protein, a marker protein of DNA damage response, was increased. In conclusion, inhibition of CDK1 by miR-195-5p overexpression may trigger replication-related DNA damage response, leading to DNA repair failure.

In a word, CDK1 has an oncogenic modulatory impact on HCC. MiR-195-5p could modulate HCC cell cycle through targeting CDK1, induce DNA damage response, and inhibit DNA replication and cell proliferation of HCC cells. These results provided a deeper understanding of function of miR-195-5p/CDK1 in HCC.

Declarations

Author contribution

Chunhui Zhou: Conceptualization, Methodology, Software, Data curation, Writing- Original draft preparation.

Sujuan Zhu: Visualization, Investigation, Supervision, Validation.

Haiping Li: Writing- Reviewing and Editing.

Declaration of Conflicting Interests

The authors report no conflict of interest.

Ethics approval and consent to participate

Not applicable.

Funding

No Fundation.

Data Availability Statement

The datasets generated and analyzed during the current study are not publicly available, but are available from the corresponding author on reasonable request.

References

1. Santamaria, D. *et al.* Cdk1 is sufficient to drive the mammalian cell cycle. Nature **448**, 811–815, doi:10.1038/nature06046 (2007).
2. Garnier, D., Loyer, P., Ribault, C., Guguen-Guillouzo, C. & Corlu, A. Cyclin-dependent kinase 1 plays a critical role in DNA replication control during rat liver regeneration. Hepatology **50**, 1946–1956,

doi:10.1002/hep.23225 (2009).

3. Johnson, N. *et al.* Cdk1 participates in BRCA1-dependent S phase checkpoint control in response to DNA damage. Mol Cell **35**, 327–339, doi:10.1016/j.molcel.2009.06.036 (2009).
4. Chow, J. P., Poon, R. Y. & Ma, H. T. Inhibitory phosphorylation of cyclin-dependent kinase 1 as a compensatory mechanism for mitosis exit. Mol Cell Biol **31**, 1478–1491, doi:10.1128/MCB.00891-10 (2011).
5. Sung, W. W. *et al.* High nuclear/cytoplasmic ratio of Cdk1 expression predicts poor prognosis in colorectal cancer patients. BMC Cancer **14**, 951, doi:10.1186/1471-2407-14-951 (2014).
6. Willder, J. M. *et al.* Androgen receptor phosphorylation at serine 515 by Cdk1 predicts biochemical relapse in prostate cancer patients. Br J Cancer **108**, 139–148, doi:10.1038/bjc.2012.480 (2013).
7. Danhier, F., Ucakar, B., Magotteaux, N., Brewster, M. E. & Preat, V. Active and passive tumor targeting of a novel poorly soluble cyclin dependent kinase inhibitor, JNJ-7706621. Int J Pharm **392**, 20–28, doi:10.1016/j.ijpharm.2010.03.018 (2010).
8. Jin, J. *et al.* LINC00346 Acts as a Competing Endogenous RNA Regulating Development of Hepatocellular Carcinoma via Modulating CDK1/CCNB1 Axis. Front Bioeng Biotechnol **8**, 54, doi:10.3389/fbioe.2020.00054 (2020).
9. Xu, T. *et al.* MicroRNA-195 suppresses tumorigenicity and regulates G1/S transition of human hepatocellular carcinoma cells. Hepatology **50**, 113–121, doi:10.1002/hep.22919 (2009).
10. Ozata, D. M. *et al.* The role of microRNA deregulation in the pathogenesis of adrenocortical carcinoma. Endocr Relat Cancer **18**, 643–655, doi:10.1530/ERC-11-0082 (2011).
11. Zhang, Q. Q. *et al.* MicroRNA-195 plays a tumor-suppressor role in human glioblastoma cells by targeting signaling pathways involved in cellular proliferation and invasion. Neuro Oncol **14**, 278–287, doi:10.1093/neuonc/nor216 (2012).
12. Li, D. *et al.* Analysis of MiR-195 and MiR-497 expression, regulation and role in breast cancer. Clin Cancer Res **17**, 1722–1730, doi:10.1158/1078-0432.CCR-10-1800 (2011).
13. Huang, D. P. *et al.* Bioinformatics Analyses of Potential miRNA-mRNA Regulatory Axis in HBV-related Hepatocellular Carcinoma. Int J Med Sci **18**, 335–346, doi:10.7150/ijms.50126 (2021).
14. Yang, W. *et al.* Accumulation of cytoplasmic Cdk1 is associated with cancer growth and survival rate in epithelial ovarian cancer. Oncotarget **7**, 49481–49497, doi:10.18632/oncotarget.10373 (2016).
15. Piao, J. *et al.* High expression of CDK1 and BUB1 predicts poor prognosis of pancreatic ductal adenocarcinoma. Gene **701**, 15–22, doi:10.1016/j.gene.2019.02.081 (2019).
16. Wu, C. X. *et al.* Blocking CDK1/PDK1/beta-Catenin signaling by CDK1 inhibitor RO3306 increased the efficacy of sorafenib treatment by targeting cancer stem cells in a preclinical model of hepatocellular carcinoma. Theranostics **8**, 3737–3750, doi:10.7150/thno.25487 (2018).
17. Xu, H. *et al.* MicroRNA-195-5p acts as an anti-oncogene by targeting PHF19 in hepatocellular carcinoma. Oncol Rep **34**, 175–182, doi:10.3892/or.2015.3957 (2015).

18. Johnson, N. *et al.* Compromised CDK1 activity sensitizes BRCA-proficient cancers to PARP inhibition. Nat Med **17**, 875–882, doi:10.1038/nm.2377 (2011).

Figures

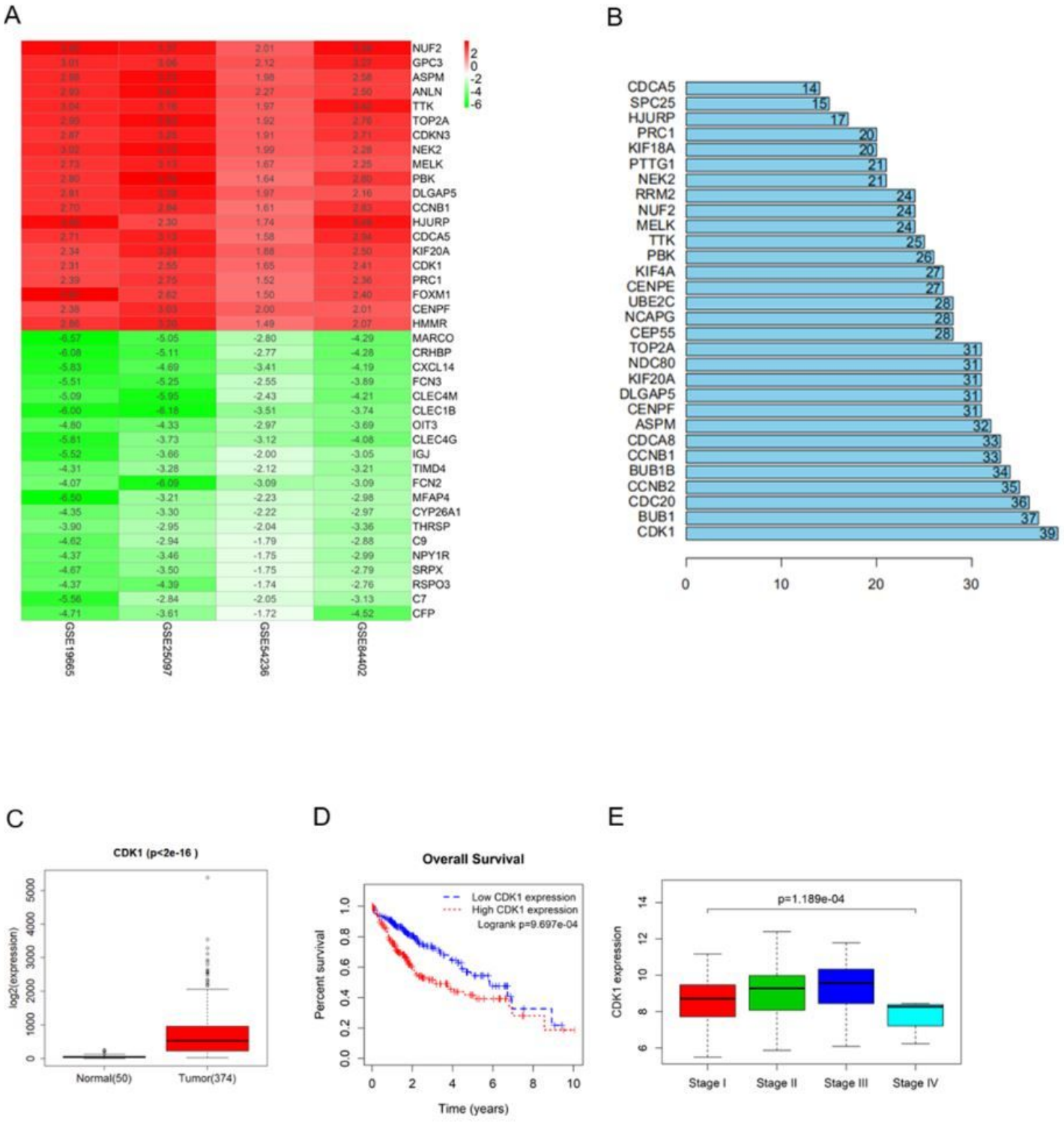

Figure 1

CDK1 may be a target of HCC

A. Heat map of the top 20 differentially expressed genes in multi-microarrays combined analysis; B. Degree statistics in gene PPI network graph (abscissa: degree value; ordinate: gene name); C. Box plot of CDK1 level in the normal and the tumor groups; D. Impact of CDK1 level on overall survival curve of patients; E. Box plot of CDK1 level in different tumor stages.

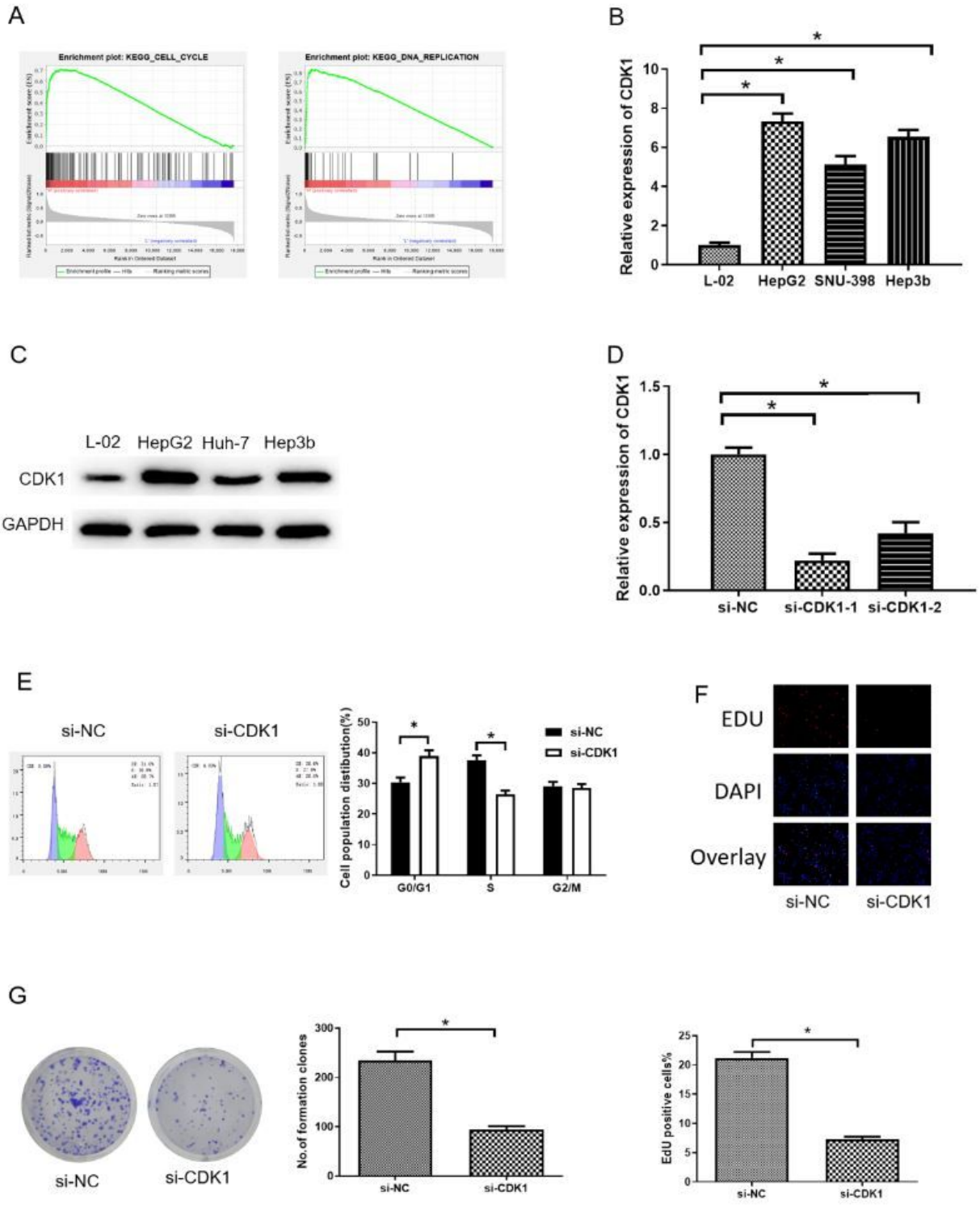

Figure 2

CDK1 regulates cell cycle, DNA replication and proliferation of HCC cells

A. Pathway enrichment results of CDK1 in GSEA; B. CDK1 RNA expression in normal human hepatocytes L-02 and HCC cell lines (HepG2, Huh-7, Hep3b) detected via qRT-PCR; C. CDK1 protein expression in normal human hepatocytes L-02 and HCC cell lines (HepG2, Huh-7, Hep3b) assessed through Western blot; D. Silencing efficiency of CDK1 assayed via qRT-PCR; E. Cell cycle assessed via flow cytometry; F. DNA replication detected by EDU staining; G. Cell proliferation detected by cell colony formation. * $p<0.05$.

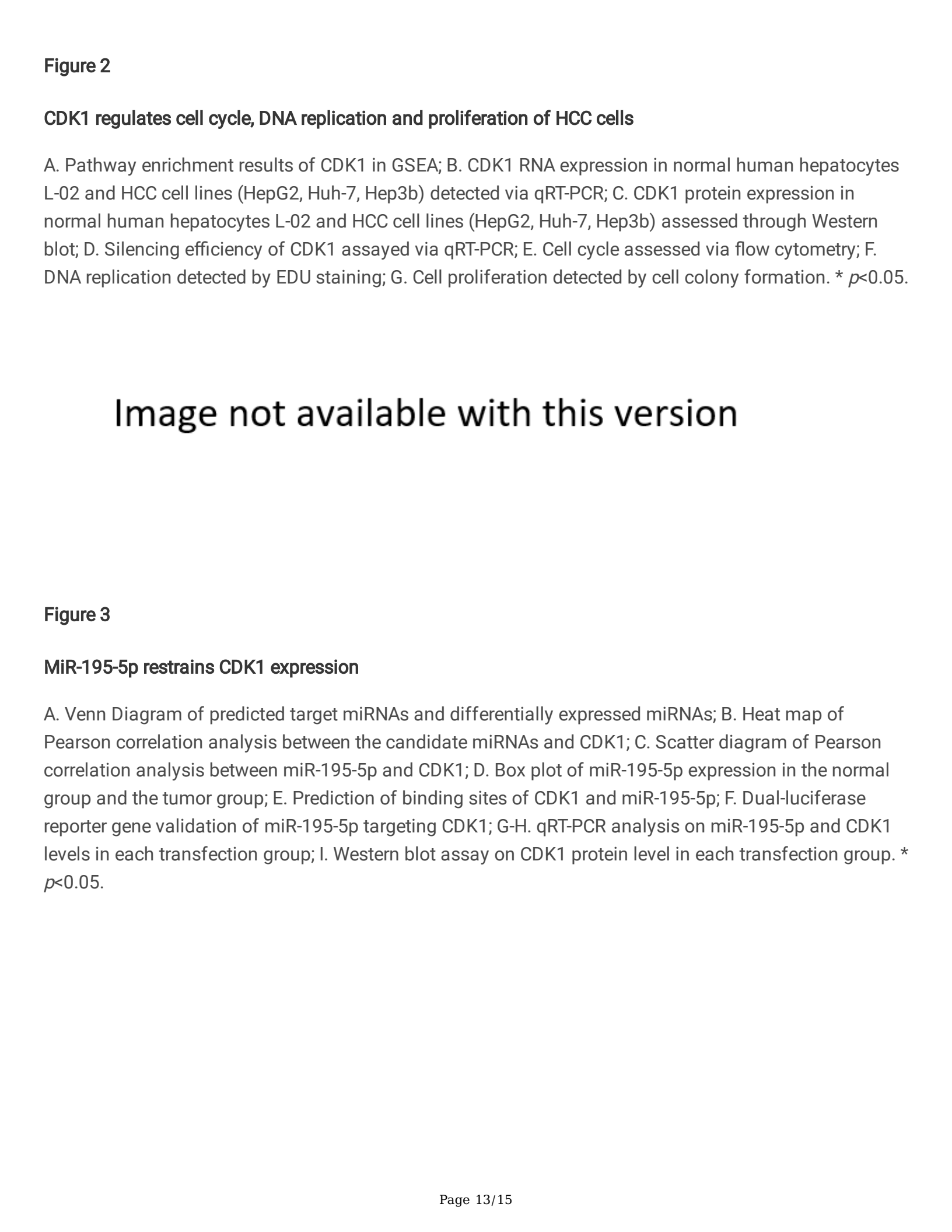

Figure 3

MiR-195-5p restrains CDK1 expression

A. Venn Diagram of predicted target miRNAs and differentially expressed miRNAs; B. Heat map of Pearson correlation analysis between the candidate miRNAs and CDK1; C. Scatter diagram of Pearson correlation analysis between miR-195-5p and CDK1; D. Box plot of miR-195-5p expression in the normal group and the tumor group; E. Prediction of binding sites of CDK1 and miR-195-5p; F. Dual-luciferase reporter gene validation of miR-195-5p targeting CDK1; G-H. qRT-PCR analysis on miR-195-5p and CDK1 levels in each transfection group; I. Western blot assay on CDK1 protein level in each transfection group. * $p<0.05$.

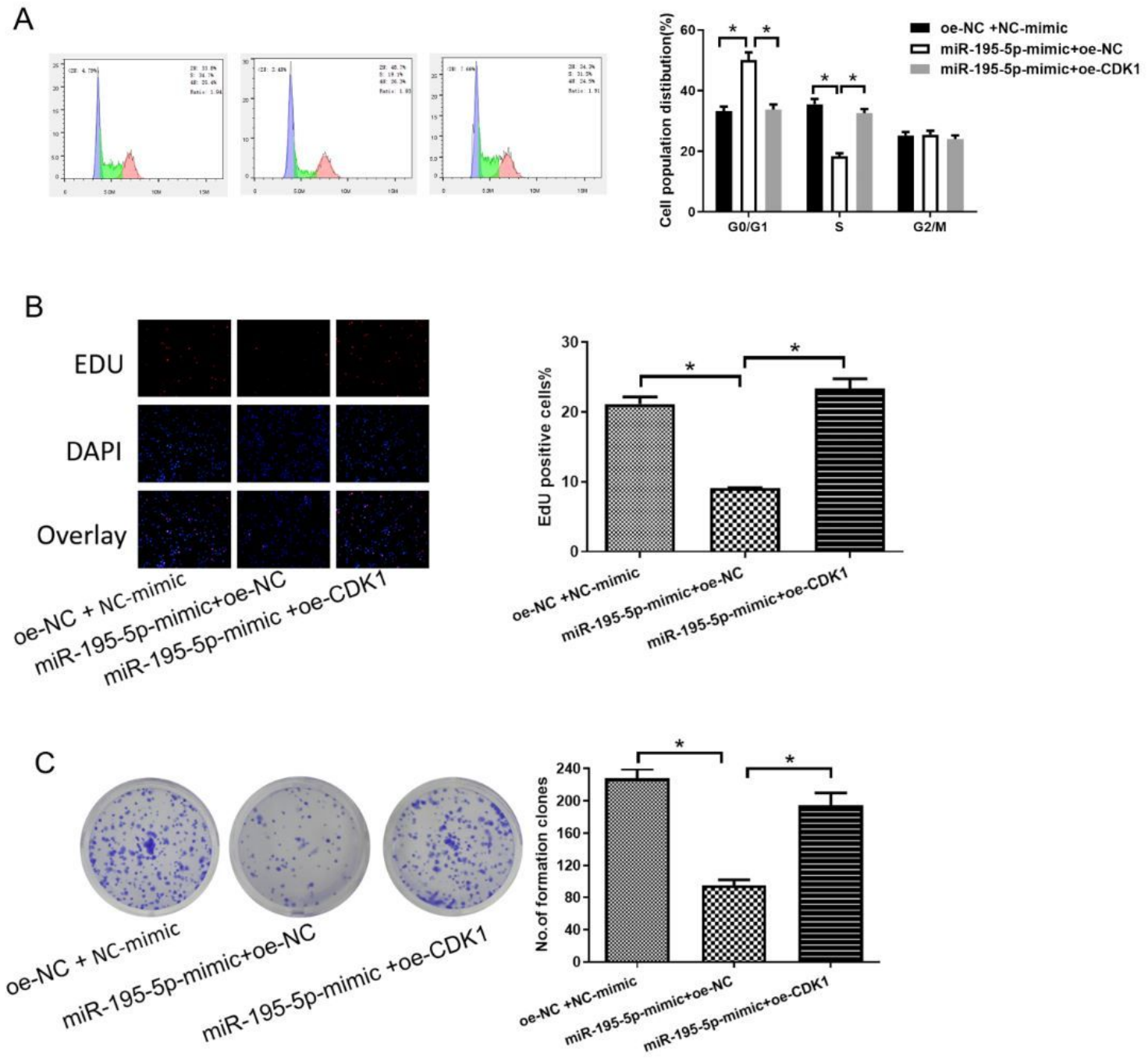

Figure 4

MiR-195-5p affects cell cycle, DNA replication and proliferation of HCC cells through targeting CDK1

A. Flow cytometry analysis on the cell cycle of each transfection group; B. EDU staining results on DNA replication; C. Cell colony formation assay results on the cell proliferative ability. * p<0.05.

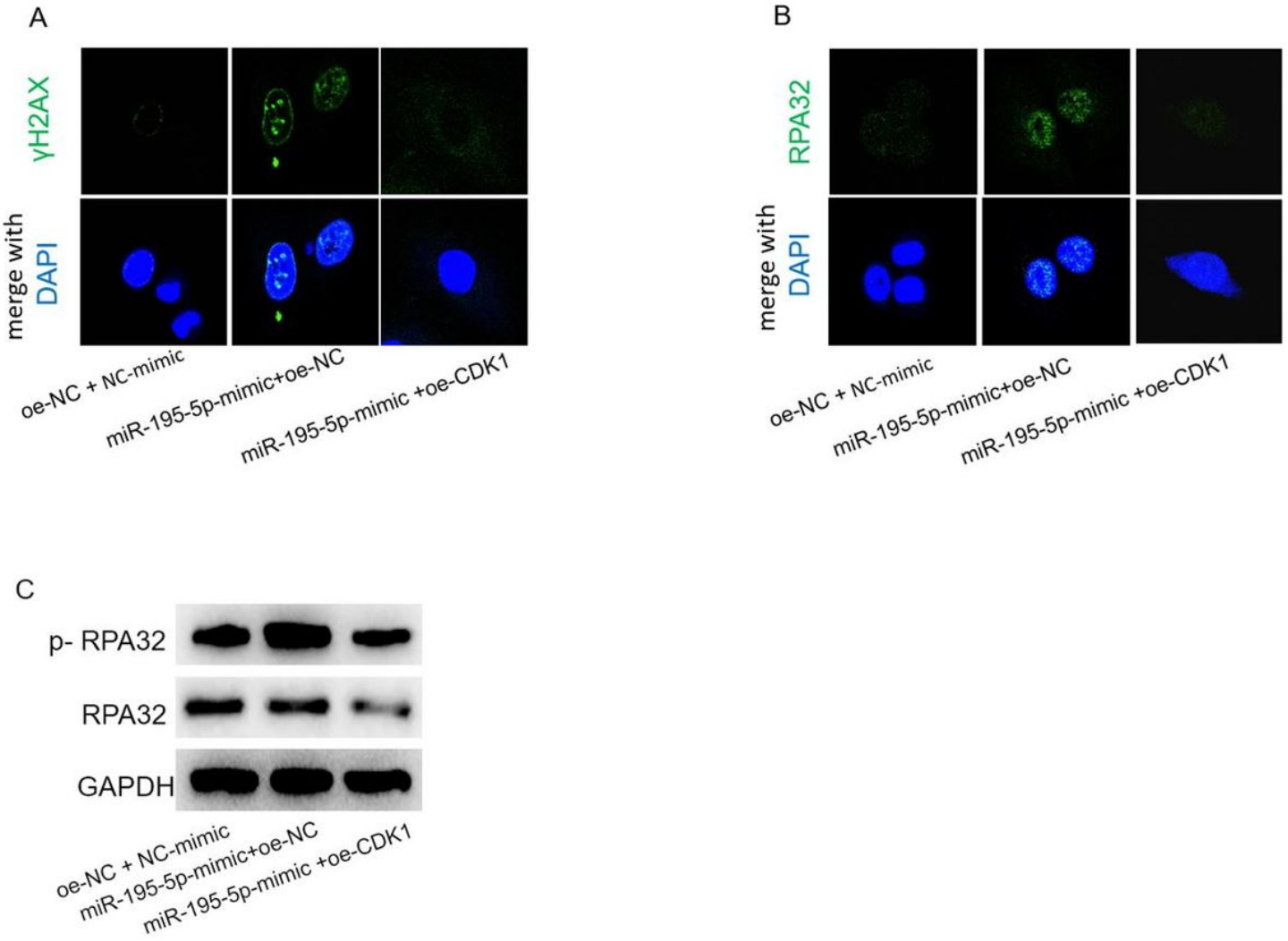

Figure 5

MiR-195-5p promotes DNA damage response in HCC

A. The γH2AX protein was labeled by immunofluorescence staining; B. The RPA32 protein was labeled by immunofluorescence staining; C. RPA32 and p-RPA32 protein levels were detected via Western blot. * $p<0.05$.